uPAR promotes formation of the p130Cas–Crk complex to activate Rac through DOCK180

Harvey W. Smith, Pierfrancesco Marra, and Christopher J. Marshall

Cancer Research UK Centre for Cell and Molecular Biology, Institute of Cancer Research, London SW3 6JB, England, UK

The urokinase-type plasminogen activator receptor (uPAR) drives tumor cell membrane protrusion and motility through activation of Rac; however, the pathway leading from uPAR to Rac activation has not been described. In this study we identify DOCK180 as the guanine nucleotide exchange factor acting downstream of uPAR. We show that uPAR cooperates with integrin complexes containing β_3 integrin to drive formation of the p130Cas–CrkII signaling complex and activation of Rac, resulting in a Rac-driven elongated-mesenchymal morphology, cell motility, and invasion. Our findings identify a signaling pathway underlying the morphological changes and increased cell motility associated with uPAR expression.

Introduction

The urokinase-type plasminogen activator receptor (uPAR) is overexpressed in many human cancers, its expression often correlating with poor prognosis (Memarzadeh et al., 2002; Kaneko et al., 2003; El-Kott et al., 2004; Salajegheh et al., 2005; Meng et al., 2006; for review see Bene et al., 2004). It is expressed as a glycosylphosphatidylinositol (GPI)-anchored plasma membrane protein and in a soluble form that is secreted or shed from the cell surface (Pedersen et al., 1993; Pyke et al., 1993; Blasi and Carmeliet, 2002). Through binding to its ligands, the protease uPA and the extracellular matrix glycoprotein vitronectin, uPAR may be involved in several processes related to tumor progression, including growth factor signaling (Liu et al., 2002; Chaurasia et al., 2006; Jo et al., 2006), release of sequestered growth factors from the ECM (Saksela and Rifkin, 1990; Sato et al., 1990; Ribatti et al., 1999), and reemergence from tumor cell dormancy (for review see Aguirre-Ghiso, 2007). Importantly, expression of uPAR is associated with the acquisition of a motile, invasive tumor cell phenotype, a process thought to be crucial for cancer metastasis (Vial et al., 2003; Lester et al., 2007; Madsen et al., 2007).

GPI-anchored uPAR localizes to the leading edge of migrating cells, and complexes of uPA–uPAR are thought to promote cell motility by activating the plasminogen system to degrade ECM (Blasi and Carmeliet, 2002; Dano et al., 2005). In addition to its roles in the regulation of pericellular proteolysis, a large body of evidence has identified uPAR as a signaling receptor that activates intracellular pathways. Activation of the Rho family small GTPase Rac has emerged as an important event in the promotion of motility and invasion by uPAR (Kjoller and Hall, 2001; Vial et al., 2003). Ectopic uPAR expression results in Rac-dependent lamellipodial protrusion and cell motility (Kjoller and Hall, 2001; Jo et al., 2003), and inhibiting endogenous uPAR expression inactivates Rac and strongly inhibits lamellipodial protrusion and cell motility (Ma et al., 2002; Vial et al., 2003). Rac activation by uPAR can occur in the absence of uPA, but depends on binding to vitronectin (Kjoller and Hall, 2001; Ma et al., 2002; Madsen et al., 2007). However, uPA binding may contribute to signaling by increasing the affinity of uPAR for vitronectin (Sidenius et al., 2002; Madsen et al., 2007). Because the vitronectin-binding site is located on the opposite side of the molecule from the uPA-binding cleft, multimeric complexes containing all three molecules may form (Llinas et al., 2005; Madsen et al., 2007).

Being GPI anchored and lacking transmembrane and cytoplasmic domains, uPAR relies on transmembrane coreceptors for intracellular signaling. Potential coreceptors for uPAR include G protein–coupled receptors (Resnati et al., 2002), tetraspanins (Bass et al., 2005), low density lipoprotein receptor-related protein (Czekay et al., 2001), and Endo180/UPARAP (Behrendt et al., 2000). In particular, several studies suggest that integrins

The Rockefeller University Press $30.00
J. Cell Biol. Vol. 182 No. 4   777–790
www.jcb.org/cgi/doi/10.1083/jcb.200712050

JCB   **777**

THE JOURNAL OF CELL BIOLOGY

are involved in uPAR signaling. Expression of uPAR results in integrin-associated signaling events such as phosphorylation of FAK and Src family kinases (Aguirre Ghiso, 2002; Zhang et al., 2003; Wei et al., 2007). uPAR–integrin interactions have been shown by coimmunoprecipitation of uPAR with leukocyte integrin Mac-1 (Simon et al., 1996), fibronectin receptors $\alpha_3\beta_1$ and $\alpha_5\beta_1$ (Wei et al., 2001; Wei et al., 2005), and vitronectin receptors $\alpha_v\beta_3$ and $\alpha_v\beta_5$ (Carriero et al., 1999; Degryse et al., 2005). The formation of these uPAR–integrin interactions may depend both on integrin subunit expression and composition of the ECM (Xue et al., 1997). Association of uPAR with integrins has been proposed to alter integrin conformation (Wei et al., 2005). However, the existence of direct uPAR–integrin binding remains controversial, as a recent study has shown that the putative integrin-binding residues in uPAR are dispensable (Madsen et al., 2007). These authors proposed that uPAR interacts indirectly with integrins by increasing cell matrix adhesion through uPAR–vitronectin binding, therefore facilitating integrin binding to ligands.

Of particular interest in the context of cell motility is how uPAR signals to Rac activation. Cycling of small GTPases between active GTP-bound and inactive GDP-bound forms is regulated by guanine nucleotide exchange factors (GEFs), which catalyze the exchange of GDP for GTP (Bos et.al. 2007), and GTPase activating proteins (GAPs), which stimulate the intrinsic GTPase activity (for review see Jaffe and Hall, 2005). Because many studies link uPAR to integrin signaling, we used a candidate approach to identify integrin-associated GEFs that might be required for Rac activation in uPAR-expressing cell lines. These studies identified DOCK180 as the GEF involved in uPAR-mediated Rac activation. We then investigated how uPAR influences signaling to DOCK180.

Results

DOCK180 is required for uPAR-driven Rac activation and invasion

Because uPAR may signal together with integrins, we examined the role of GEFs that have been linked to integrin signaling to identify GEFs that may function downstream of uPAR. A literature search identified α-PIX, β-PIX, DOCK180, Sos1, Tiam1, Tiam2, Vav1, Vav2, and Vav3 as potential Rac GEFs downstream of integrins (Kiyokawa et al., 1998; Moores et al., 2000; Marignani and Carpenter, 2001; Matsuo et al., 2003; Rosenberger et al., 2003; Arthur et al., 2004; Gakidis et al., 2004; Faccio et al., 2005; Hamelers et al., 2005). We used RNAi to silence expression of these GEFs (apart from α-PIX, Vav1, and Vav3 for which no expression was detected) in the colon carcinoma cell line BE. BE cells endogenously express uPAR and exhibit a bipolar mesenchymal morphology with abundant membrane ruffling and lamellipodia shown by phalloidin staining to be F-actin rich (Fig. 1 A). This characteristic morphology, together with extensive random migration, is abrogated by silencing uPAR or Rac (Vial et al., 2003). We used this easily scorable phenotype to search for GEFs whose silencing mimicked the effects of silencing uPAR. DOCK180 was the only GEF for which silencing resulted in similar effects to abrogating uPAR expression, resulting in
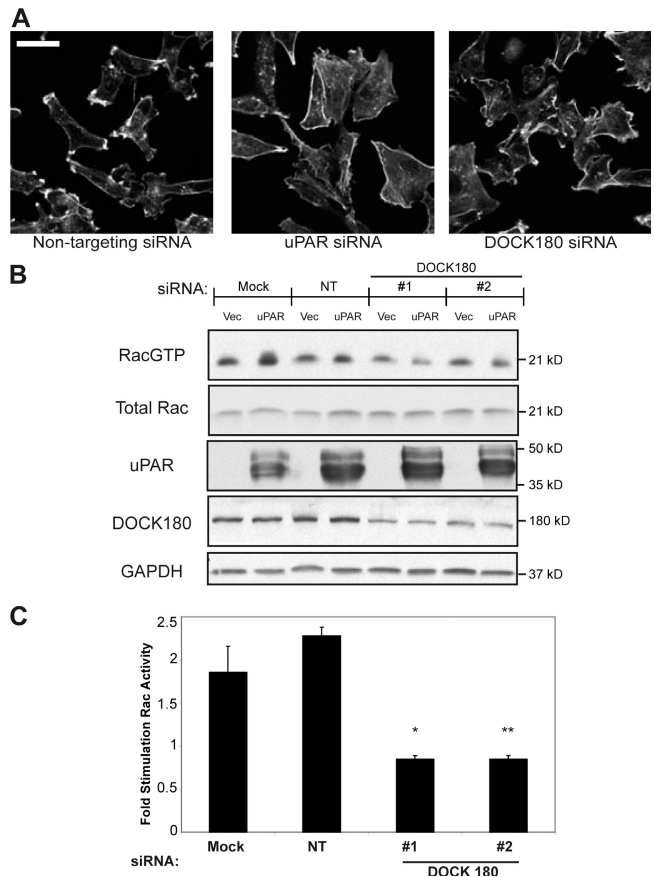
Figure 1. **DOCK180 is required for uPAR-driven membrane ruffling and Rac activation.** (A) BE colon carcinoma cells transfected with indicated siRNAs were plated on vitronectin-coated coverslips for 12 h, fixed, and stained with Texas red–conjugated phalloidin. Bar, 50 µm. (B and C) HEK 293T cells were transfected with siRNAs targeting DOCK180 or non-targeting control (NT), and 48 h later were transfected with uPAR expression vector or empty vector control. After 24 h, Rac-GTP pull-down assays were performed. (B) Representative immunoblots to show pull-down assay, uPAR expression, and DOCK180 silencing. (C) Rac activation was quantitated and analyzed as described in Materials and methods (mean + SEM; $n = 3$). *, $P < 0.05$; **, $P < 0.01$; unpaired Student's t test.

flattening, loss of ruffles and lamellipodia, more pronounced cortical actin staining, and occasional stress fibers (Fig. 1 A and Fig. S1 A, available at http://www.jcb.org/cgi/content/full/jcb.200712050/DC1).

To show that uPAR signals through DOCK180 to activate Rac, we used ectopic expression in human embryonic kidney (HEK) 293T cells that lack endogenous uPAR. Transfection with a uPAR expression construct activates Rac approximately twofold (Fig. 1, B and C). Strikingly, this stimulation was lost when uPAR was expressed in HEK 293T cells in which DOCK180 expression had been abrogated with either of two different siRNAs (Fig. 1, B and C). Significantly, in empty vector controls, DOCK180 silencing had no effect on Rac activity, showing basal Rac activity in HEK 293T cells does not require DOCK180. Therefore, in this system DOCK180 is required for uPAR-driven Rac activation rather than basal levels of Rac activity.

To examine whether DOCK180 is required for Rac activation in tumor cell lines expressing uPAR, we used BE, MDA-MB-231 breast carcinoma cells, and SNB19 glioblastoma cells in which

endogenous uPAR signaling is required for cell motility or invasion (Mohan et al., 1999; Sturge et al., 2002; Vial et al., 2003). We silenced DOCK180 expression in these cell lines using a panel of siRNA oligonucleotides, including an ON-TARGET SMART pool that incorporates technology designed to reduce "off-target" effects. Each siRNA treatment abrogating DOCK180 expression significantly reduced Rac activation (Fig. 2 A). The degree of inhibition of Rac activation resulting from silencing DOCK180 was very similar to that from silencing uPAR (∼50–60%; Fig. 2 A). As well as reducing Rac activation, siRNA treatments against either DOCK180 or uPAR elicited similar morphological changes in the three cell lines with reduced membrane ruffling and lamellipodial protrusion (Fig. S1 B and not depicted), demonstrating that the effects are a true consequence of silencing these genes rather than a nonspecific or off-target effect.

Because uPAR-driven Rac activation has been shown to promote invasion (Vial et al., 2003), BE and MDA-MB-231 cells were assayed for invasion of a three-dimensional collagen matrix in response to a chemotactic gradient of serum. Fig. 2 B shows that in both cell lines silencing DOCK180 or uPAR inhibited invasion to a comparable degree (40–50%). Confirming that loss of Rac reduced cell motility, time-lapse phase-contrast microscopy revealed a severe defect in random cell motility when DOCK180 or uPAR was silenced (Videos 1–3 [BE], available at http://www.jcb.org/cgi/content/full/jcb.200712050/DC1; and not depicted for MDA-MB-231 and SNB19).

These studies show that in an ectopic uPAR expression system and in three different tumor cell lines expressing endogenous uPAR, silencing DOCK180 results in reduced Rac activation. This suggests that uPAR signals through DOCK180 for uPAR-driven Rac activation and membrane protrusion, resulting in cell motility and invasion.

uPAR drives tyrosine phosphorylation of p130Cas and formation of the Cas–Crk complex

Because uPAR signals through DOCK180 to activate Rac, the roles of known upstream regulators of DOCK180 were examined to characterize the pathway linking uPAR and DOCK180. The regulation of DOCK180 by integrin signaling involves protein–protein interactions where the N-terminal SH3 domain of the adaptor protein Crk binds to a proline-rich region in DOCK180 (Matsuda et al., 1996) and the SH2 domain of Crk binds to phosphotyrosine residues in the substrate domain (SD) of the adaptor p130Cas (Sakai et al., 1994). The p130Cas–Crk–DOCK180 module associates with integrins via binding of p130Cas to FAK (Polte and Hanks, 1995). To investigate whether uPAR influences p130Cas SD tyrosine phosphorylation and recruitment of Crk, we first examined the effects of ectopic uPAR expression in HEK 293T cells. Expression of uPAR results in an ∼50% increase in tyrosine phosphorylation of the p130Cas SD (Fig. 3 A). Increased tyrosine phosphorylation of p130Cas was associated with a dramatic induction of the p130Cas–Crk complex, as determined by coimmunoprecipitation of Crk and p130Cas (Fig. 3 B). These results show that ectopic expression of uPAR drives formation of the p130Cas–Crk complex. As the p130Cas SD has been shown to be phosphorylated by Src family kinases
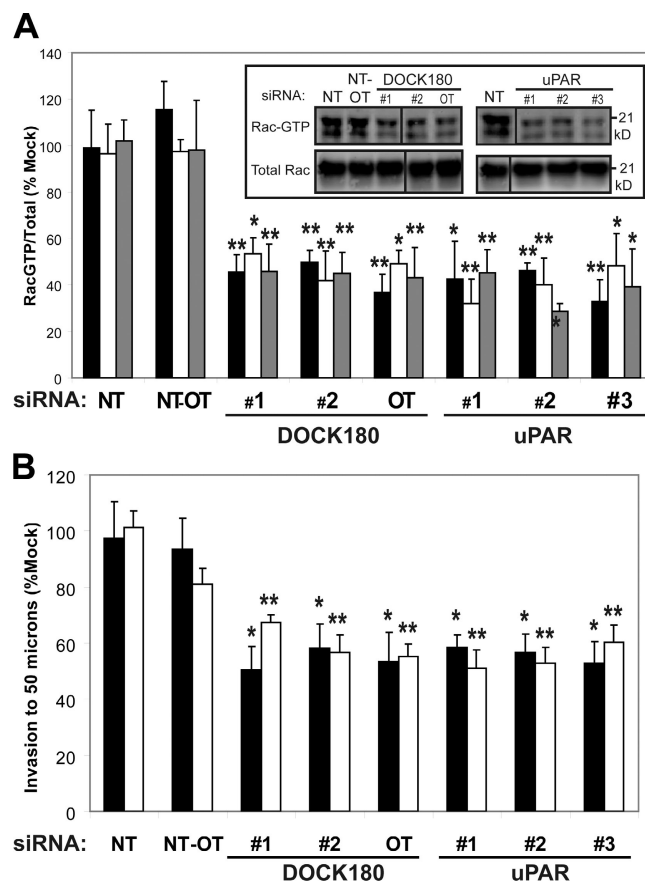

Figure 2. **DOCK180 is required for Rac activation and invasion in uPAR-expressing tumor cell lines.** (A) BE (closed bars), MDA-MB-231 (open bars), and SNB19 (shaded bars) cells were transfected with siRNAs. NT, nontargeting control; NT-OT, ON-TARGET nontargeting control. Rac activity was quantitated at 72 h (mean + SEM; $n \geq 3$). *, $P < 0.05$; **, $P < 0.01$; unpaired Student's t test. (inset) Representative immunoblots from one Rac pull down in BE cells. Irrelevant lanes were removed (represented by vertical black lines). (B) BE (closed bars) and MDA-MB-231 (open bars) cells transfected with siRNAs were assayed for collagen-I invasion (mean + SEM; $n \geq 3$). *, $P < 0.05$; **, $P < 0.01$; unpaired Student's t test. Immunoblots showing knockdown are in Fig. S2 A, available at http://www.jcb.org/cgi/content/full/jcb.200712050/DC1.

(Vuori et al., 1996), and as uPAR has been linked to c-Src activity (Zhang et al., 2003), we investigated whether uPAR-dependent Rac activation required c-Src activity. Ectopic expression of uPAR in HEK 293T cells led to increased c-Src phosphorylation on the Y416 activation site and treatment with the Src inhibitors PP1 or PP2 or the structurally unrelated SU6656 blocked Rac activation, whereas PP3, the inactive stereoisomer of PP2, had no effect (Fig. S3 A, available at http://www.jcb.org/cgi/content/full/jcb.200712050/DC1).

To examine whether endogenously expressed uPAR signals through p130Cas and Crk, we silenced uPAR expression in the tumor cell lines. Silencing uPAR with each of three different siRNA oligonucleotides reduced p130Cas SD tyrosine phosphorylation by up to 40% in each cell line (Fig. 3 C). Similar results were observed in SNB19 and MDA-MB-231 cells (unpublished data). In all three tumor cell lines, the formation of the p130Cas–Crk complex was also strongly inhibited by silencing uPAR (Fig. 3 D).

Figure 3. uPAR expression drives p130Cas SD phosphorylation and formation of the p130Cas–CrkII complex. (A) p130Cas SD tyrosine phosphorylation in uPAR- or vector-transfected (Vec) HEK 293T cells. Left, representative immunoblots; right, quantitation of SD phosphorylation (mean + SEM; $n = 3$). (B) p130Cas–Crk complex formation in uPAR- or empty vector–transfected HEK 293T cells. Left, representative immunoblots; right, immunoblot showing expression of p130Cas, uPAR, and GAPDH. (C) p130Cas SD tyrosine phosphorylation in siRNA-transfected cells. Top left, representative immunoblots (BE); top right, uPAR immunoblotting; bottom, quantitation. Closed bars, BE; open bars, MDA-MB-231; shaded bars, SNB19 cells (mean + SEM; $n = 4$). *, $P < 0.05$; **, $P < 0.01$; unpaired Student's t test. (D) Analysis of p130Cas–Crk complex formation. Left, representative immunoblots (BE); right, quantitation. Closed bars, BE cells; open bars, MDA-MB-231 cells; shaded bars, SNB19 cells (mean + SEM; $n \geq 4$). *, $P < 0.05$; **, $P < 0.01$; unpaired Student's t test.
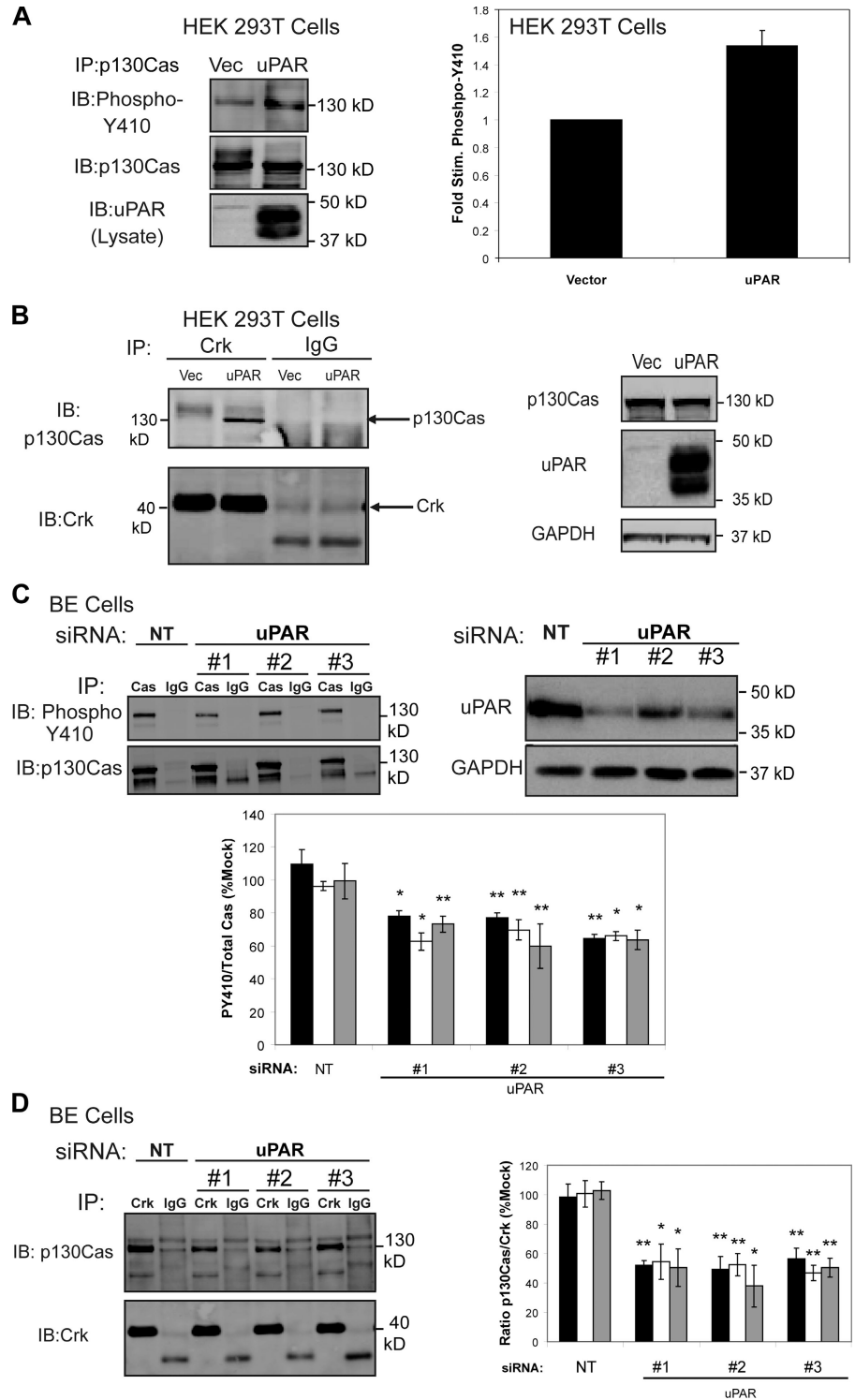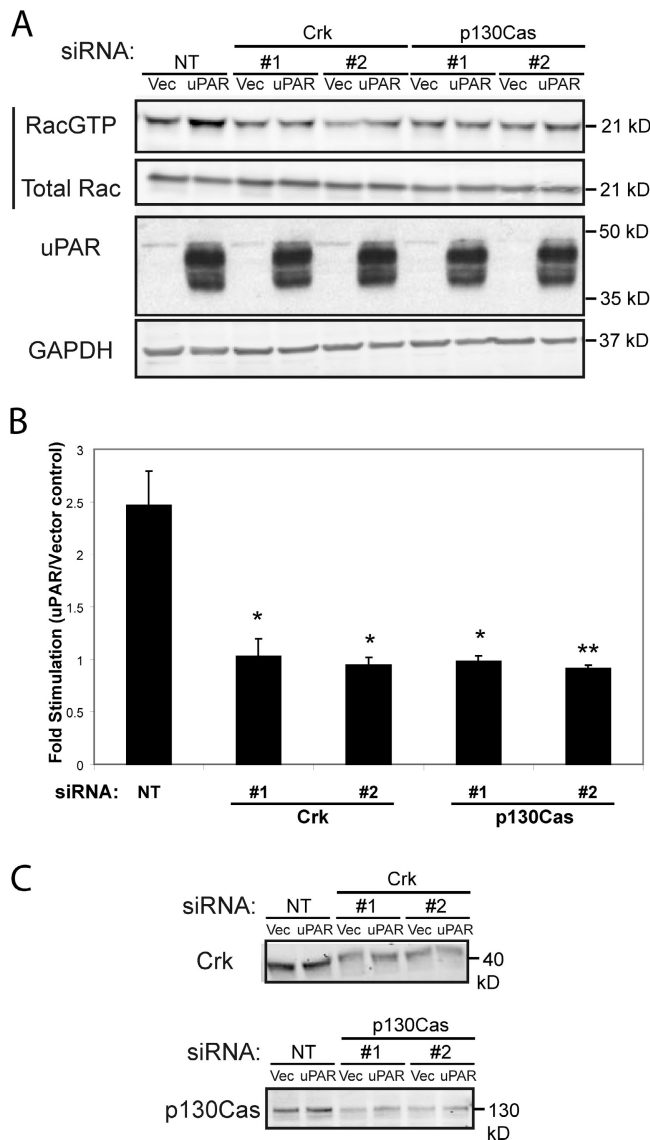

To confirm that p130Cas and Crk are required for uPAR signaling to Rac activation, we used the ectopic uPAR expression system. Silencing p130Cas or Crk abrogated the 2–2.5-fold stimulation of Rac-GTP loading on uPAR expression in HEK 293T cells (Fig. 4, A and B). As with DOCK180 silencing (Fig. 1, B and C), silencing p130Cas or Crk did not affect basal Rac-GTP loading, demonstrating the specific role of p130Cas and Crk in uPAR signaling to Rac. Consistent with the findings from the ectopic expression studies, silencing the expression of

either adaptor using three different siRNA oligonucleotides, including ON-TARGET SMART pools, in the endogenous uPAR-expressing tumor cell lines BE and SNB19 resulted in ~50–60% inhibition of Rac activity (Fig. 5 A).

These results argue that uPAR activates Rac through driving the formation of p130Cas–Crk complexes that could potentially recruit DOCK180 through association with Crk. To confirm that signaling through uPAR can recruit DOCK180 to complexes containing p130Cas, we immunoprecipitated DOCK180 and
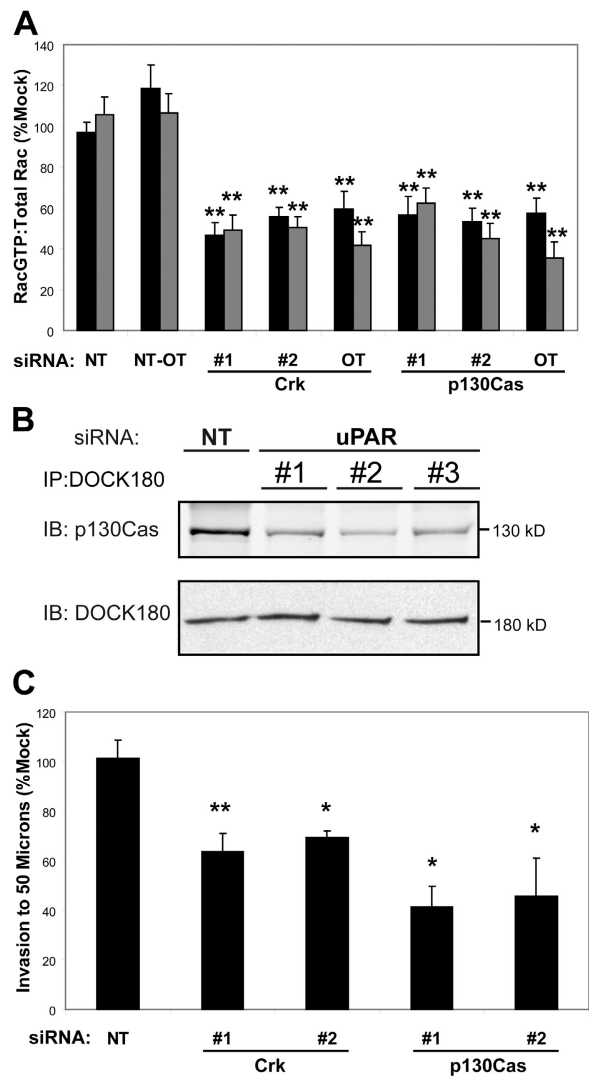
Figure 4. **p130Cas and Crk are required for uPAR-stimulated Rac activation in HEK 293T cells.** HEK 293T cells were transfected with siRNAs. 48 h after siRNA transfection cells were transfected with uPAR expression vector or empty vector control (Vec). 24 h later (72 h after siRNA transfection), Rac pull-down assays were performed. (A) Representative immunoblots from one experiment. (B) Quantitation of Rac activation (mean + SEM; n = 3). *, P < 0.05; **, P < 0.01; unpaired Student's t test. (C) Representative immunoblots of silencing p130Cas and CrkII at 72 h after transfection.

Figure 5. **p130Cas and Crk are required for Rac activation and invasion in uPAR-expressing tumor cell lines.** (A) BE cells (closed bars) and SNB19 cells (shaded bars) were transfected with siRNAs, and Rac activation was quantitated as described in Fig. 2 (mean + SEM; n ≥ 5). **, P < 0.01; unpaired Student's t test. (B) BE cells were transfected with siRNAs, and the association of p130Cas with DOCK180 was determined by immunoprecipitation of DOCK180 and immunoblotting for p130Cas. Immunoblots are representative of three independent experiments. (C) BE cells were transfected with siRNAs. At 60 h after transfection, cells were assayed for collagen-I invasion (mean + SEM; n ≥ 4). *, P < 0.05; **, P < 0.01; unpaired Student's t test. Immunoblots showing knockdown are in Fig. S2 B, available at http://www.jcb.org/cgi/content/full/jcb.200712050/DC1.

blotted for p130Cas. Fig. 5 B shows that in BE cells, p130Cas and DOCK180 coimmunoprecipitate but the amount of this complex is reduced when uPAR is silenced. This indicates that DOCK180 and the adaptor proteins p130Cas and Crk are in the same pathway downstream of uPAR rather than in separate pathways (Tosello-Trampont et al., 2007).

To demonstrate that p130Cas–Crk complex signaling to Rac contributes to tumor cell invasion, we studied whether abrogating expression of p130Cas or Crk affects BE cell invasion of a three-dimensional collagen matrix. Fig. 5 C shows that silencing p130Cas or Crk inhibited invasion by ∼40–50%. Silencing p130Cas or Crk has similar effects on Rac activation (Fig. 1 C) or inva-

sion (Fig. 2 B) to when either uPAR or DOCK180 is silenced (Fig. 2, A and B).

Requirement for β₃ integrin in uPAR-driven Rac activation

Our data show that uPAR expression drives tyrosine phosphorylation of the p130Cas SD, promoting the formation of the p130Cas–Crk complex that recruits DOCK180. This leads to Rac activation and acquisition of a motile, invasive phenotype in tumor cell lines. Because the p130Cas–Crk–DOCK180 pathway is known to be activated by integrin-mediated adhesion (Kiyokawa et al., 1998), we investigated which integrins are involved.
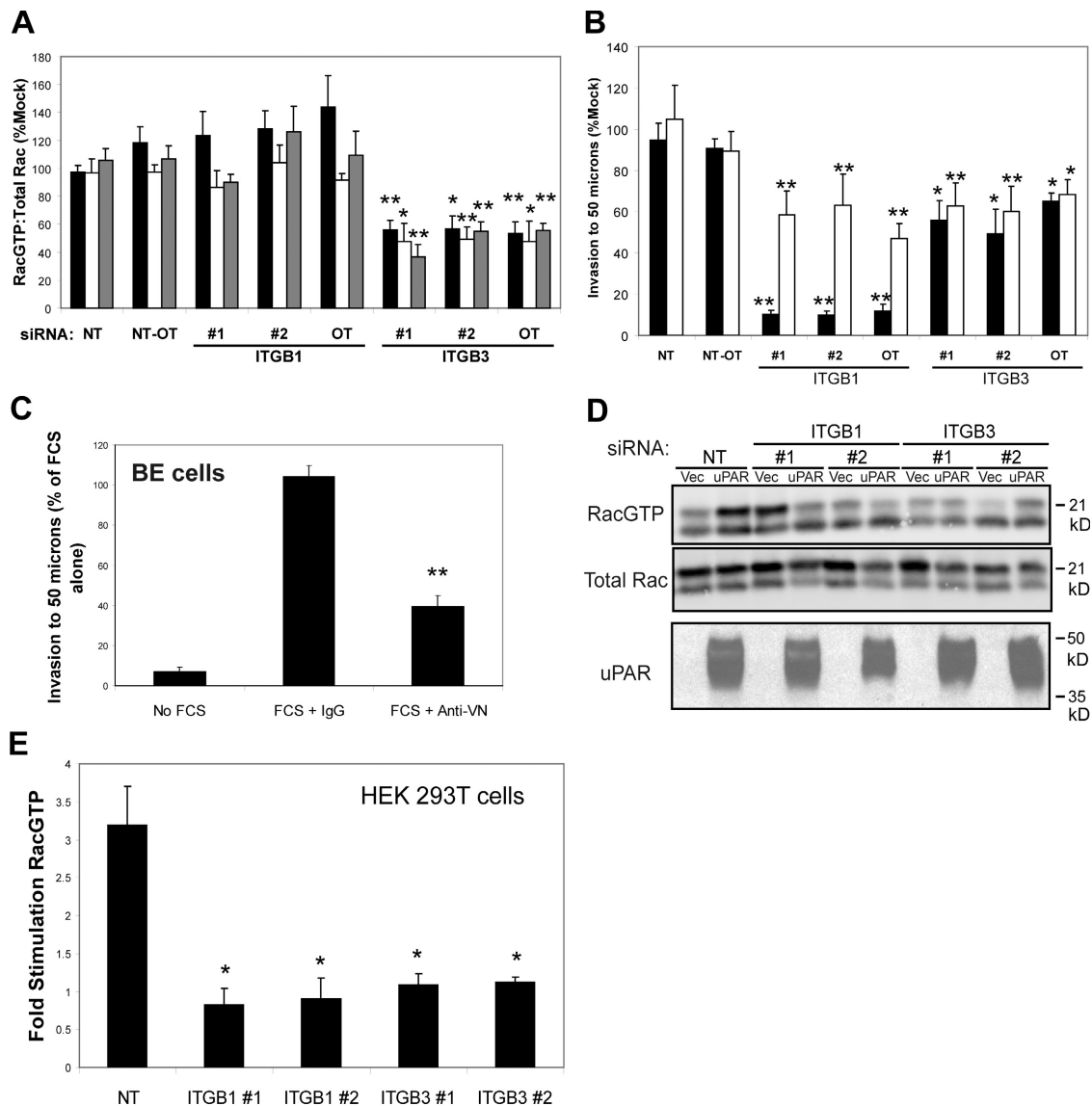
Figure 6. **β₃ integrin is required for Rac activation in uPAR-expressing cells.** (A) Tumor cells were transfected with siRNAs and Rac activation was quantitated. Closed bars, BE; open bars, MDA-MB-231; shaded bars, SNB19 (mean + SEM; $n \geq 4$). *, $P < 0.05$; **, $P < 0.01$; unpaired Student's t test. (B) BE (closed bars) and MDA-MB-231 cells (open bars) were transfected with siRNAs and assayed for collagen-I invasion (mean + SEM; $n \geq 4$). *, $P < 0.05$; **, $P < 0.01$; unpaired Student's t test. (C) BE cells were seeded for invasion assays in serum-free DME or DME + 5% serum and either control IgG or antivitronectin antibody (mean + SEM; $n \geq 4$). **, $P < 0.01$; unpaired Student's t test. (D) HEK 293T cells were transfected with siRNAs, and after 48 h, transfected with uPAR or empty vector. Rac activity was measured 24 h later. (E) Quantitation of Rac-activation assays in HEK 293T cells (mean + SEM; $n \geq 5$). *, $P < 0.05$; unpaired Student's t test versus nontargeting. Immunoblots showing knockdown are in Fig. S2 (C and D), available at http://www.jcb.org/cgi/content/full/jcb.200712050/DC1.

BE, MDA-M231, and SNB19 cells express $\alpha_v\beta_3$, $\alpha_v\beta_5$, and β_1 integrin (see Fig. 7 D; Fig. S5 D, available at http://www.jcb.org/cgi/content/full/jcb.200712050/DC1; and not depicted), which have been reported to interact with uPAR (Carriero et al., 1999; Degryse et al., 2005; Chaurasia et al., 2006). Blocking antibody and siRNA experiments showed that $\alpha_v\beta_3$ and $\alpha_v\beta_5$, but not uPAR, are required for adhesion to vitronectin (Fig. S5, A–C). To investigate the involvement of integrins in uPAR signaling to Rac activation, β integrin subunits were silenced using panels of siRNA oligonucleotides consisting of two individual oligonucleotide duplexes and one ON-TARGET SMART pool for each target (ITGB1#1, ITGB1#2, and ITGB1 OT for targeting β_1 integrin; ITGB3#1, ITGB3#2, and ITGB3 OT for targeting β_3 integrin; and ITGB5#1, ITGB5#2, and ITGB5 OT for targeting β_5 integrin). Only silencing of β_3 integrin mimicked the phenotype of uPAR or DOCK180 silencing in BE cells (Fig. S4, A and B). Similar effects were observed in MDA-MB-231 and SNB19 cells (unpublished data). Silencing β_1 integrin resulted in loss of polarity and delocalization of membrane ruffling whereas silencing β_5 resulted in defects in adhesion and rear retraction (Fig. S4, A and B).

Rac pull-down assays showed that silencing β_3 integrin but not β_1 integrin in BE, MDA-MB-231, and SNB19 cells decreased Rac activation (Fig. 6 A). Consistent with the lack of an effect on membrane ruffling, silencing β_5 integrin had no effect on Rac activation (Fig. S4 C). The effect of silencing β_3 integrin

is very similar in magnitude to that observed when uPAR, DOCK180, Crk, or p130Cas is silenced. Consistent with the fact that $\alpha_v\beta_3$ is a major vitronectin receptor (Cheresh and Spiro, 1987), we found that silencing uPAR or β_3 integrin only affected Rac activity in BE cells plated on vitronectin and not on collagen or fibronectin, which are major β_1 integrin ligands (Fig. S5 E). Similarly, ectopic expression of uPAR in HEK 293T cells led to Rac activation if the cells were plated in serum-free medium on vitronectin or in serum as a source of vitronectin, but there was no Rac activation if the cells were plated in serum-free medium on fibronectin or collagen-1 (Fig. S5 F).

The contributions of signaling through β_1 and β_3 integrin subunits to invasion were examined by testing β_1- and β_3-silenced BE and MDA-MB-231 cells for invasion of a three-dimensional collagen-1 matrix (Fig. 6 B). In both BE and MDA-MB-231 cells, silencing β_3 integrin inhibited invasion by ~40%. Invasion in these assays was dependent on vitronectin present in serum as no invasion took place in the absence of serum, and the addition of a vitronectin-blocking antibody (Zanetti et al., 1994) blocked serum-dependent invasion (Fig. 6 C). This was consistent with the observed effects on invasion of silencing uPAR, DOCK180, Crk, and p130Cas in these cells. Although it did not affect Rac activation, silencing β_1 integrin decreased invasion by ~90% in BE cells and 40–50% in MDA-MB-231 cells. This is not unexpected because all collagen-binding integrins contain the β_1 subunit, and adhesion to the substratum is essential for the elongated/mesenchymal mode of migration (Pollard and Borisy, 2003).

To investigate whether β_3 integrin was required for uPAR-driven Rac activation in HEK 293T cells, integrin subunits were silenced with siRNA; Fig. 6 (D and E) shows that silencing β_3 in HEK 293T cells blocked Rac activation. However, unlike the tumor cell lines, β_1 silencing did reduce Rac activation in uPAR-transfected HEK 293T cells. Significantly, flow cytometry showed that $\alpha_v\beta_3$ was not expressed at the surface of control or empty vector–transfected HEK 293T cells but was expressed at the surface of uPAR-transfected cells (Fig. 7 A). Previous work has shown that sustained extracellular signal–regulated kinase (ERK) activation leads to surface expression of β_3 integrin (Woods et al., 2001), and as uPAR-mediated ERK activation has been shown to be β_1 dependent (Aguirre Ghiso et al., 1999), we examined whether β_1 integrin expression and ERK activation were required for surface expression of β_3. Fig. 7 A shows that silencing β_1 integrin or treatment with the MAPK/ERK kinase (MEK) inhibitors PD184352 or UO126 (unpublished data) blocked surface expression of $\alpha_v\beta_3$ in uPAR-transfected HEK 293T cells. Silencing β_1 integrin but not β_3 integrin blocked uPAR-dependent ERK activation, showing that ERK activation by uPAR requires β_1 but not β_3 integrin (Fig. 7 B). Consistent with the observations that β_1 integrin signals to ERK activation and surface expression of $\alpha_v\beta_3$, inhibition of ERK activation with MEK inhibitors PD184352 or UO126 blocked Rac activation in uPAR-transfected HEK 293T cells (Fig. 7 C). These results show that signaling via uPAR and β_1 integrins to ERK activation can provide the surface localization of $\alpha_v\beta_3$ required for uPAR-dependent Rac activation. Although β_1 integrin–dependent ERK activation was required for surface expression of β_3 integrin,

immunoblotting showed that uPAR expression, β_1 integrin knockdown, or inhibition of ERK activation did not affect total cell levels of β_3 integrin (Fig. 7 A).

In contrast to HEK 293T cells, uPAR or β_1 integrin silencing in BE colon carcinoma cells did not affect the surface localization of $\alpha_v\beta_3$ integrin (Fig. 7 D); however, surface expression of $\alpha_v\beta_3$ integrin in BE, MDA-MB231, and SNB19 was partially dependent on ERK activation (Fig. 7 D and Fig. S5 D). In none of the tumor cell lines was β_1 integrin or uPAR required for ERK activation (Fig. 7 E). BE and MDA-MB231 harbor activating mutations in KRAS and BRAF or KRAS alone (Vial et al., 2003) that presumably uncouple ERK activation from a requirement for β_1 integrin and uPAR. These results therefore argue that uPAR signals through $\alpha_v\beta_3$ for Rac activation, but that uPAR signaling through β_1 integrins can provide an ERK signal for surface localization of $\alpha_v\beta_3$.

β_3 integrin is required for p130Cas SD tyrosine phosphorylation and formation of the p130Cas–CrkII complex

Because β_3 integrin–silenced cells had defects in morphology, Rac activation, and invasion similar to those observed in cells where components of the uPAR–DOCK180 pathway had been silenced, we examined the roles of β integrin subunits in signaling through the p130Cas–CrkII adaptor complex. Silencing β_3 integrin in BE, MDA-MB231, and SNB19 tumor cells strongly reduced tyrosine phosphorylation of the p130Cas SD (Fig. 8 A). Conversely, silencing β_1 integrin did not affect p130Cas SD phosphorylation. In keeping with the p130Cas SD tyrosine phosphorylation data, coimmunoprecipitation of p130Cas with CrkII was also inhibited by silencing β_3 integrin, whereas silencing of β_1 integrin had no effect (Fig. 8 B). These data show that expression of uPAR promotes signaling through β_3 integrin to drive tyrosine phosphorylation of the p130Cas SD and formation of the p130Cas–CrkII adaptor complex. Consistent with the requirement for Src in Rac activation driven by uPAR, silencing β_3 integrin blocked Src activation driven by uPAR (Fig. S3, B and D) but did not affect FAK Y397 phosphorylation (Fig. S3 C). Silencing β_3 integrin also abrogated the stimulation of p130Cas SD tyrosine phosphorylation by ectopically expressed uPAR in HEK 293T cells (Fig. 8 C). However, as observed for uPAR-driven Rac activation, silencing β_1 integrin in HEK 293T cells also abrogated uPAR-driven p130Cas SD tyrosine phosphorylation. This is consistent with the role of β_1 integrin in promoting cell surface expression of β_3 integrin by cooperating with uPAR to activate ERK, a function of β_1 integrin that is not required in the tumor cells where ERK activity does not require β_1 integrin (Fig. 7 E).

Discussion

In this study we have identified a mechanism of Rac activation by uPAR. We show for the first time that in both ectopic and endogenous systems uPAR expression results in activation of Rac via the GEF DOCK180. DOCK180 has been shown to have a role in cell motility (Klemke et al., 1998) and developmental processes such as myoblast fusion, dorsal closure, and phagocytosis
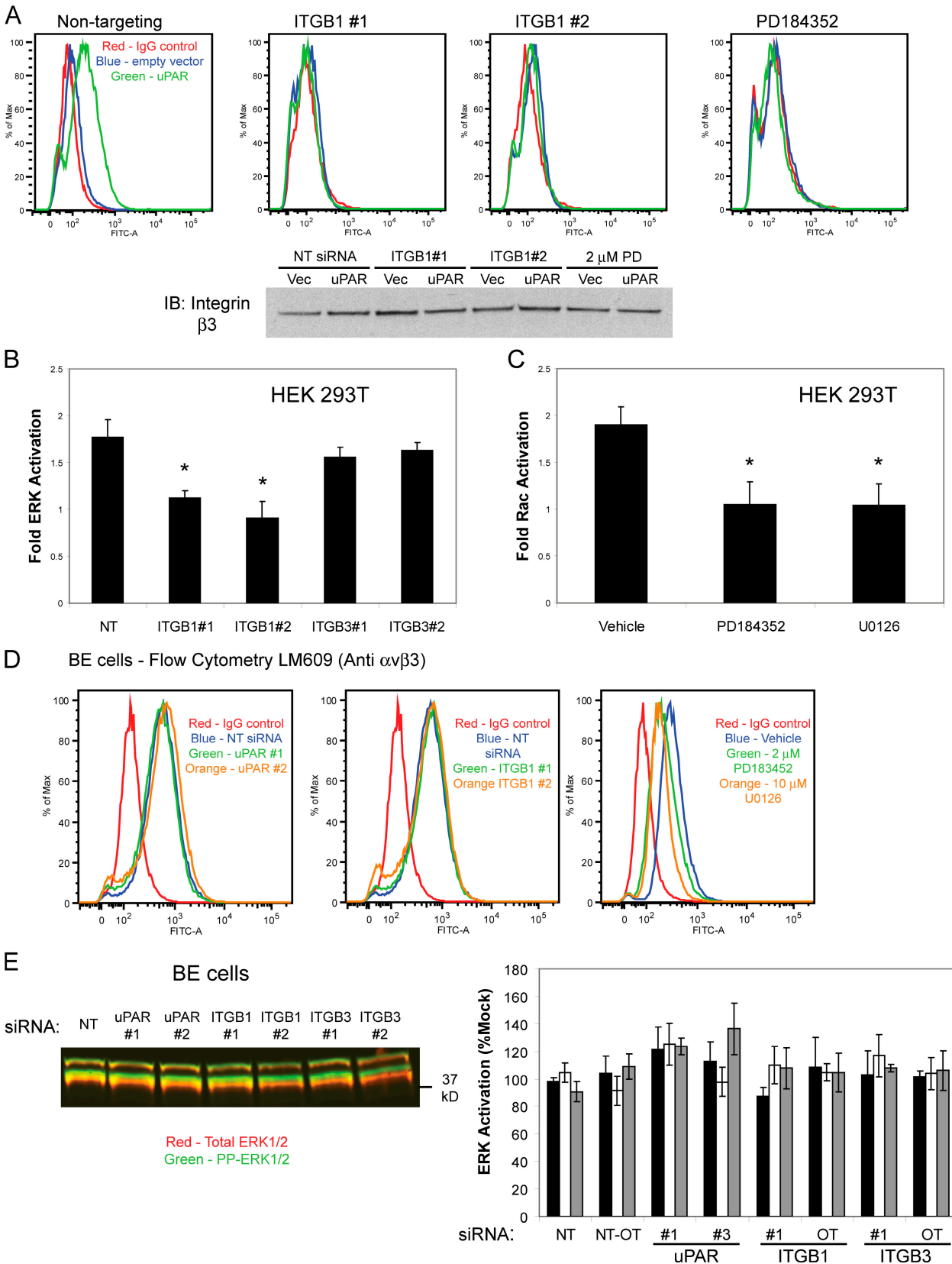
Figure 7. **Cooperation between uPAR signaling with β₁ integrin to ERK-MAPK activation and β₃ integrin–dependent Rac activation.** (A) Cell surface expression of $\alpha_v\beta_3$ in uPAR- or vector-transfected HEK 293T cells. Top three left panels, siRNA-transfected cells; top right panel, 2 µM PD184352 or vehicle (DMSO) treatment. Red, IgG control; blue, $\alpha_v\beta_3$ vector transfected; green, uPAR–$\alpha_v\beta_3$ transfected. (bottom) β_3 integrin immunoblot of siRNA-transfected or PD184352-treated HEK 293T cells. (B) HEK 293T cells were transfected as in A and ERK1/2 activation was measured (mean + SEM; $n = 6$). *, $P <$ 0.05; unpaired Student's t test. (C) Rac activation in HEK 293T cells transfected with uPAR or vector and treated with MEK inhibitors or vehicle (DMSO)

of apoptotic cells (Nolan et al., 1998; Wu and Horvitz, 1998; Moore et al., 2007). Our data show that uPAR signaling to DOCK180 results in the induction of tumor cell motility and invasion. In several systems, ELMO has been linked to DOCK180 function possibly through acting as a cofactor for GEF activity (Gumienny et al., 2001; Brugnera et al., 2002). Whether it is involved in uPAR-driven Rac activation will be an interesting topic for future investigation.

Having identified DOCK180 as a Rac GEF regulated by uPAR, we examined how DOCK180 is activated downstream of uPAR. Previous work in other systems shows that integrin signaling recruits DOCK180 to the plasma membrane via the formation of a p130Cas–Crk–DOCK180 complex. Key to the formation of this complex is tyrosine phosphorylation of the p130Cas SD that recruits Crk–DOCK180 complexes via the SH2 domain of Crk. We show that uPAR, expressed endogenously by tumor cells or ectopically in HEK 293T cells, drives the tyrosine phosphorylation of the p130Cas SD and formation of the p130Cas–Crk complex. For Rac activation by uPAR, uPA does not seem to be essential (Kjoller and Hall 2001) and is not expressed by HEK 293T cells (Wei et al., 1994). However, uPA–uPAR interactions may play an important role in other systems or in tumor cell invasion in vivo, whether by enhancing uPAR binding to vitronectin or through mechanisms such as focused ECM proteolysis at the leading edge or enhancing local availability of growth factors. Consistent with uPAR signaling through the p130Cas–Crk complex, we find that p130Cas and Crk are required for Rac activation by uPAR and for the invasion of uPAR-expressing tumor cells.

p130Cas is a multifunctional adaptor protein required for embryonic development and oncogenic signal transduction in tumor cells (Auvinen et al., 1995; Nievers et al., 1997; Honda et al., 1998; Kirsch et al., 2002; Cabodi et al., 2006). It is also an important regulator of cell migration, and in particular its association with Crk constitutes a molecular switch vital for cell motility by recruiting DOCK180 to integrin-containing adhesion complexes (Klemke et al., 1998). These complexes also serve a mechanosensory function allowing the cell to sense the physical properties, such as rigidity, of the ECM (for review see Bershadsky et al., 2006). Interestingly, in vitro data suggests that p130Cas can function as a transducer of mechanical signals, with the SD adopting an extended conformation permissive for phosphorylation in response to increased physical force (Sawada et al., 2006). This could promote Rac-driven migration in response to physical cues in the extracellular environment. As we have shown that uPAR stimulates the tyrosine phosphorylation of the p130Cas SD, the role of uPAR in integrin-mediated mechanotransduction is an interesting subject for future investigation. In addition, it is well known that p130Cas and Crk can interact with other partners besides DOCK180. Therefore, promotion of p130Cas SD tyrosine phosphorylation and p130Cas–CrkII

complex assembly by uPAR may regulate a variety of other signaling pathways.

The identification of DOCK180, an integrin-associated GEF, in uPAR-Rac signaling is in keeping with a large body of evidence implicating integrins as the signaling partners of uPAR. A relatively large array of integrin heterodimers have been shown to interact with uPAR, but whether any of these are specifically required for uPAR to activate Rac in tumor cells had not been previously investigated. In the tumor cell lines we examined, β_3 but not β_1 integrin was required for uPAR–DOCK180 signaling to Rac activation. In HEK 293T cells, β_1 as well as β_3 integrin are required for uPAR-stimulated Rac activation, but in these cells the role of β_1 integrin appears to be to provide the ERK activation (Aguirre-Ghiso et al., 1999) necessary for surface expression of $\alpha_v\beta_3$. Thus, in some cells uPAR–β_1 integrin signaling to ERK-dependent surface expression of $\alpha_v\beta_3$ cooperates with uPAR–$\alpha_v\beta_3$ signaling for Rac activation, whereas in other cells uPAR–β_3 integrin drives Rac activation but ERK activation does not seem to require uPAR or β_1 integrin signaling.

Several papers have emphasized the importance of vitronectin in membrane protrusion and cell motility induced by uPAR expression, and both integrin signaling and direct binding of uPAR to vitronectin were recently shown to be required for stimulation of membrane ruffling and lamellipodial protrusion by ectopic uPAR expression in HEK 293T cells (Kjoller and Hall, 2001; Madsen et al., 2007). We have shown that uPAR and β_3 integrin are required for Rac activation in tumor cells cultured on vitronectin or in the presence of serum, which is an abundant source of vitronectin with concentrations in the range of 200 to 400 µg/ml (Schvartz et al., 1999). In the collagen-1–based three-dimensional invasion assay we have used, a function-blocking antivitronectin antibody inhibits serum-stimulated invasion, demonstrating that invasion is dependent on vitronectin. Consistent with its role in uPAR-driven Rac activation in the presence of vitronectin, silencing β_3 integrin expression also inhibits serum-stimulated invasion.

These data suggest that uPAR and β_3 integrin engage vitronectin to promote Rac activity and tumor cell invasion. The nature of uPAR–integrin interactions is controversial. Although many studies have shown uPAR–integrin coimmunoprecipitation, this does not prove the existence of direct binding. Immunoprecipitation under gentle conditions may result in the detection of many proteins associated with detergent-resistant lipid rafts, including uPAR and integrins. The study of Madsen et al. (2007) has cast doubt on the role of specific uPAR residues in mediating binding to integrins, although it does not rule out direct interactions involving multiple residues over a large binding surface. Our data are consistent with a model where both uPAR and β_3 integrin coordinately engage vitronectin. This could affect signaling in several ways, for example, by facilitation of integrin–ligand interaction, effects on integrin clustering, or modification of integrin

for 24 h (mean + SEM; $n = 6$). *, $P < 0.05$; unpaired Student's t test. (D) Surface expression of $\alpha_v\beta_3$ on BE cells. Left and middle, siRNA transfections; right, MEK inhibition. Data are representative of three independent experiments. (E) ERK1/2 activation in cells transfected with siRNAs. Left, representative immunoblot (BE), total ERK1/2 (red), phospho-ERK1/2 (green); right, quantitation (mean + SEM; $n = 4$). Closed bars, BE cells; open bars, MDA-MB-231; shaded bars, SNB19.
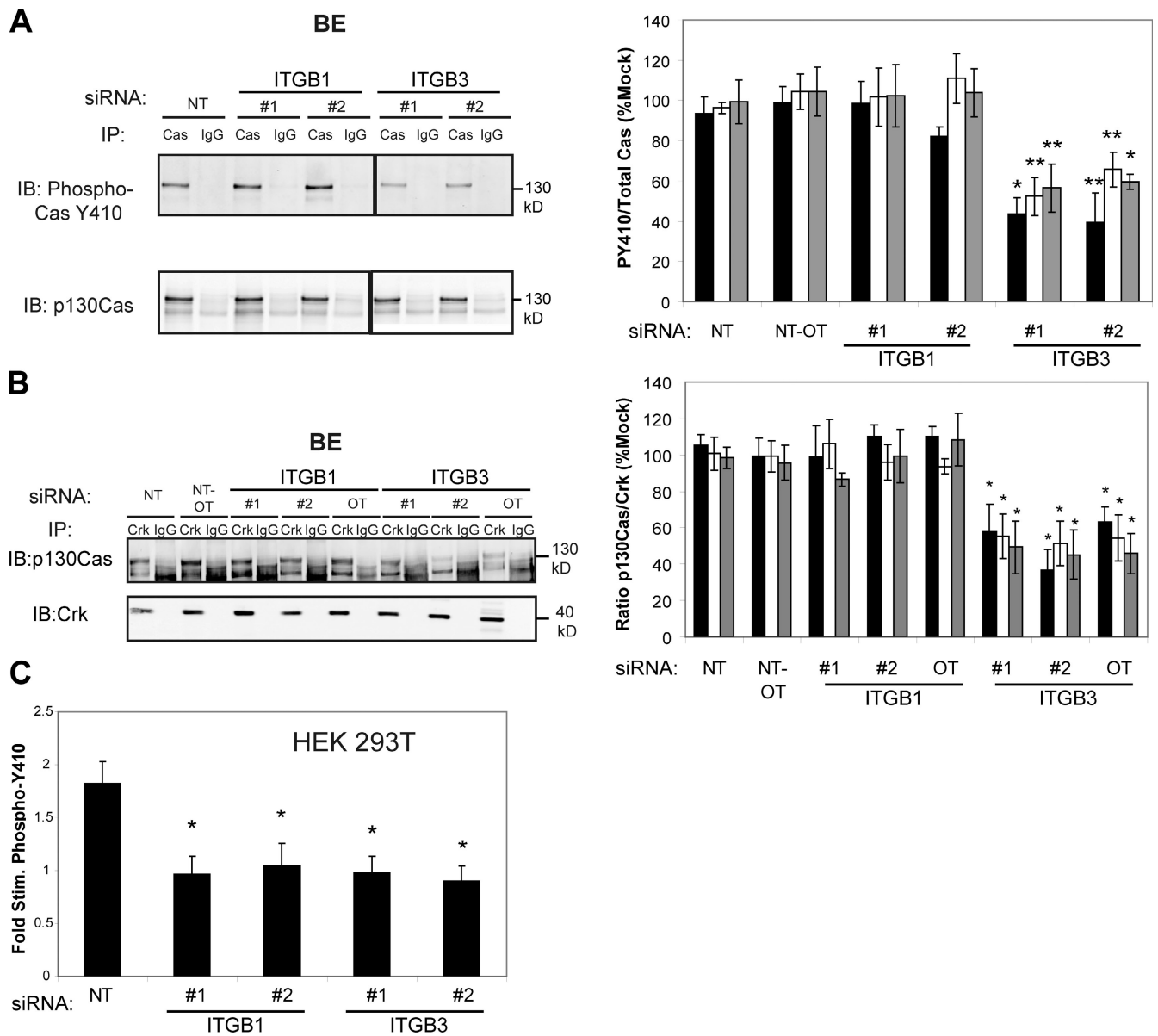
Figure 8. **β₃ integrin is required for p130Cas SD tyrosine phosphorylation and formation of the p130Cas–CrkII complex.** (A) p130Cas SD tyrosine phosphorylation in siRNA-transfected cells. Left, representative immunoblot (BE); right, quantitation (mean + SEM; $n = 5$). *, $P < 0.05$; **, $P < 0.01$; unpaired Student's *t* test. Closed bars, BE; open bars, MDA-MB-231; shaded bars, SNB19. Irrelevant lanes were removed (represented by vertical black lines). (B) Analysis of p130Cas–Crk complexes. Left, representative immunoblots (BE); right, quantitation (mean + SEM; $n = 4$). *, $P < 0.05$; unpaired Student's *t* test. Closed bars, BE; open bars, MDA-MB-231; shaded bars, SNB19. (C) Analysis of p130Cas SD tyrosine phosphorylation in HEK 293T cells transfected with siRNAs and uPAR or empty vector was performed as described in Fig. 3 (mean + SEM; $n = 4$). *, $P < 0.05$; unpaired Student's *t* test. Immunoblots showing knockdown are in Fig. S2 E, available at http://www.jcb.org/cgi/content/full/jcb.200712050/DC1.

conformation by lateral uPAR–integrin interactions. Interestingly, silencing uPAR expression or blocking uPAR function using an antibody that recognizes the vitronectin-binding site had no effect on the adhesion of tumor cells to vitronectin (Fig. S5, A–C). Significantly, while this paper was in preparation, Wei et al. (2008) have demonstrated that uPAR expression leads to the activation of β₃ integrins in the murine kidney (Wei et al., 2008).

Interestingly, our data show that β₁ integrin silencing causes a severe cell motility phenotype in uPAR-expressing tumor cell lines, without affecting Rac activation but causing a delocalization of membrane ruffling and lamellipodia. β₁ integrin signaling may affect tumor cell polarity, for example, by regulating Cdc42,

which is a major regulator of polarized migration (Etienne-Manneville, 2004). Also by inhibiting internalization of lipid rafts, which contain both uPAR and binding sites for activated Rac (del Pozo et al., 2004), and by regulating interactions with RhoGDI (Del Pozo et al., 2002), β₁ integrin may affect spatial control of Rac-driven protrusion and motility.

Determination of the molecular mechanisms underlying uPAR signaling, such as the Rac activation pathway described here, is essential to provide insight into the well-established role of uPAR in tumor cell invasion. Understanding these pathways will provide new therapeutic targets for the prevention of human tumor metastasis.

Materials and methods

Antibodies and reagents

The following antibodies were used: anti-Rac1 (clone 23A8; Fitzgerald), anti-uPAR (R&D Systems), anti-GAPDH (Novus Biologicals), anti-DOCK180, anti–$\beta_3$integrin, anti–$\beta_1$integrin (clone P5D2; Santa Cruz Biotechnology, Inc.), anti–β_1 integrin (clone JB1a), anti–β_3 integrin rabbit polyclonal, anti-$\alpha_v\beta_3$ (LM609), anti-$\alpha_v\beta_5$ (P1F6), antivitronectin (clone BV2; Millipore), anti-p130Cas, anti-Crk, anti-FAK (BD Biosciences), anti–α-tubulin, anti-total, phosphoERK (Sigma-Aldrich), anti-p130Cas phosphotyrosine 410 (Cell Signaling Technology), anti–c-Src (clone GD11; Millipore), anti-Src phosphoY416 (Invitrogen), anti-FAK phosphoY397 (Affinity Bio-Reagents), and mouse IgG isotype controls (R&D systems). Vitronectin and fibronectin (purified from human serum) were purchased from Sigma-Aldrich. Bovine Type I collagen solution was purchased from Invitrogen. PD184352 was obtained from C. Springer (Institute of Cancer Research, Sutton, England, UK) and U0126 was obtained from Sigma-Aldrich. PP1, PP2, PP3, and SU6656 were purchased from EMD). Texas red–labeled phalloidin was purchased from Invitrogen. pRcCMV-uPAR was a provided by A. Hall (Memorial Sloan-Kettering Cancer Center, New York, NY). HRP-coupled secondary antibodies were from purchased Sigma-Aldrich and fluorophore-coupled secondary antibodies were purchased from Li-COR Biosciences.

Cell culture

BE colon carcinoma cells were obtained from the Institute of Cancer Research Tissue Resource Laboratory; HEK 293T and MDA-MB-231 breast carcinoma cells from the American Tissue Type Culture Collection; and SNB19 glioblastoma cells from the Deutsche Sammlung von Mikroorganismen und Zellkulturen. All cells were maintained in DME, supplemented with 10% FCS purchased from PAA Laboratories, 100 µg/ml streptomycin, and 60 µg/ml penicillin. Cells were maintained at 37°C and 10% CO_2. siRNA transfections in tumor cell lines were performed using InterferIN (Polyplus) according to the manufacturer's instructions. The final concentration of siRNA in the transfection was 2 nM. For siRNA transfection of HEK 293T cells, HiPerfect (QIAGEN) was used with 50-nM final concentration of siRNA according to the manufacturer's instructions. Sequences of siRNA oligonucleotides were as follows: DOCK180 #1, CUGACUCAGAAC-GUGGACC; DOCK180 #2, UAAAUGAGCAGCUGUACAA; DOCK180-OT (Thermo Fisher Scientific); uPAR #1, GAAGAGACUUUCCUCAUUG; uPAR #2, GGUGACGCCUUCAGCAUGA; uPAR #3, GGUGAAGAAGGGC-GUCCAA; Crk #1, AAUAGGAGAUCAAGAGUUU; Crk #2, GGACAGC-GAAGGCAAGAGA; Crk-OT (Thermo Fisher Scientific); p130Cas #1, GGUCGACAGUGGUGUGUAU; p130Cas #2, AGAAGGAGCUGCUG-GAAAA; p130Cas-OT (Thermo Fisher Scientific); ITGB1 #1 (targeting β_1 integrin), GAACAGAUCUGAUGAAUGA; ITGB1 #2 (targeting β_1 integrin), CAAGAGAGCUGAAGACUAU; ITGB1-OT (targeting β_1 integrin; Thermo Fisher Scientific); ITGB3 #1 (targeting β_3 integrin), CUCUCCUGAUGUAG-CACUUAA; ITGB3 #2 (targeting β_3 integrin), CACGUGUGGCCU-GUUCUUCUA; ITGB3-OT (targeting β_3 integrin; Thermo Fisher Scientific); ITGB5 #1 (targeting β_5 integrin), GAACAACGGUGGAGAUUUU; ITGB5 #2 (targeting β_5 integrin), GGAGGGAGUUUGCAAAGUU; ITGB5-OT (targeting β_5 integrin; Thermo Fisher Scientific). Controls used were All-Stars nontargeting control (QIAGEN), ON-TARGET nontargeting control SMART Pool (Thermo Fisher Scientific), and nontargeting control SMART Pool (Thermo Fisher Scientific).

Transfection of HEK 293T cells with plasmid DNA (6 µg DNA per 10-cm cell culture dish) was performed using GeneJuice (EMD) according to the manufacturer's instructions. Plasmid DNA was prepared using the HiSpeed Plasmid Maxi kit (QIAGEN).

Microscopy

Static phase-contrast images were obtained from a microscope camera workstation (Digital Site DS-4; Nikon) attached to an inverted phase-contrast microscope (TS100; Nikon) using a LWD 20× objective (NA 0.4; Nikon) at 21°C. Images were processed for contrast and brightness using Photoshop v7.0 (Adobe).

Multi-site time-lapse video microscopy was performed in a humidified, CO_2-equilibrated chamber at 37°C using an inverted phase-contrast microscope (TE2000; Nikon) in conjunction with digital cameras (either Orca-ER or C9100EM-CCD; Hamamatsu Photonics), and equipped with motorized stage, focus, and shutter systems (Prior Scientific Instruments, Ltd.), all controlled by Simple PCI AIC acquisition software (v6.5; Compix Imaging Systems). Cells were imaged using PlanFluor 10× (0.3 NA; Nikon) or PlanFluor ELWD 20× (0.45 NA; Nikon) objectives for at least

24 h at a rate of one frame per site per 4 min. Movies were exported from Simple PCI software as uncompressed AVI files with a frame rate of 15 frames per second. Premiere (v6.0; Adobe) was used to compress movie files using the MPEG codec, which were then converted to MOV (Quicktime) format using iMovie HD with a frame rate of 15 frames per second (dimensions: 640 × 512).

Confocal sections were obtained with a laser-scanning confocal imaging system (MRC 1024; Bio-Rad Laboratories) mounted on an upright fluorescence microscope (E600; Nikon) with PLan Apo 60× oil immersion objective (NA 1.4) at 21°C, and using LaserSharp acquisition software (Bio-Rad Laboratories). Images were exported as PIC files and processed for brightness and contrast using Photoshop, supplemented with PIC file recognition plug-in (Bio-Rad Laboratories).

Analysis of Rac1 activation

A GST fusion of the CRIB domain of PAK1 was used to pull down the activated form of Rac (Benard et al., 1999). The PAK1-CRIB domain GST fusion protein was bound to glutathione-Sepharose beads (GE Healthcare). $5 \times 10^5 - 10^6$ cells in a 10-cm dish were washed in Rac wash buffer (50 mM Tris-HCl, 10 mM $MgCl_2$, 1 mM DTT [Sigma-Aldrich], and EDTA-free complete protease inhibitors [Roche]) and lysed on ice for 3 min in ice-cold Rac lysis buffer (50 mM Tris-HCl, 10% glycerol, 1% NP-40, 5 mM $MgCl_2$, 100 mM NaCl, and EDTA-free complete protease inhibitors). Lysates were cleared by centrifugation at 13,200 rpm for 5 min in a centrifuge (5810R; Eppendorff) at 4°C and an aliquot was kept for determination of total Rac levels by Western blotting. The remainder of the lysate was incubated with 30-µl PAK-CRIB–Sepharose beads for 45 min on a rotating wheel at 4°C. Beads were collected by brief centrifugation and washed three times in 500 µl of ice-cold Rac lysis buffer and resuspended in 20 µl of LDS sample buffer (Invitrogen), and electrophoresis (NOVEX NuPAGE Midi gel system; Invitrogen) was performed with the total volume of each Rac pull down and equivalent volumes of total cell lysate for determination of total Rac. Fluorescent immunoblotting of Rac in pull downs and total lysate used anti-Rac clone 23A8 (Fitzgerald) and the Odyssey (Li-COR Biosciences). Data from the Odyssey were exported into Excel (Microsoft) and the ratio of signals for Rac GTP/Total Rac was calculated for each sample. For tumor cell lines, data are normalized to values from mock-transfected cells. Statistical comparisons for each siRNA were made against the nontargeting control and ON-TARGET SMART Pools were compared with ON-TARGET nontargeting controls. For HEK 293T cells, data are shown as fold stimulation of Rac activation, obtained by dividing the Rac activation in uPAR-transfected cells by that of the vector control for each condition.

Invasion assay

Cells were suspended in 2.3 mg/ml of serum-free liquid bovine collagen at 10^5 cells/ml. 100-µl aliquots were dispensed into black 96-well View-Plates (PerkinElmer) coated with bovine serum albumin. Plates were centrifuged at 300 g and incubated in a 37°C/10% CO_2 tissue culture incubator. Once collagen had polymerized, FCS was added on top of the collagen to a final concentration of 5%. For vitronectin-blocking studies, 20 µg/ml antivitronectin antibody or isotype-matched IgG control were preincubated with FCS for 30 min at room temperature. After 24-h incubation at 37°C in 10% CO_2, cells were fixed and stained for 2 h in 4% formaldehyde solution (Sigma-Aldrich) containing 5 µg/ml Hoechst 33258 nuclear stain (Invitrogen). Confocal z slices were collected from each well at 50 µm to count invaded cells, and at the bottom (3 µm) to count total cells using a high content microscope (INCELL3000; GE Healthcare) with a 40× PlanFluor ELWD objective (0.6 NA; Nikon). Nuclear staining in each slice was quantified automatically with INCELL3000 Object Intensity module to determine the percentage of invaded cells. Samples were run in quadruplicate and averaged. Data analysis was performed using Excel. Invasion index was calculated at number of cells at 50 µm per total number of cells. Data are presented as a percentage of the invasion index of mock-transfected cells. Statistical comparisons for siRNAs were made against the nontargeting control, and ON-TARGET SMART Pools were compared with ON-TARGET nontargeting controls.

Immunoprecipitation and immunoblotting

Cells were grown in 10- or 15-cm plates and lysed in 1% NP-40 buffer (1% NP-40, 150 mM NaCl, 50 mM Tris-HCl, pH 7.4, 25 mM sodium β-glycerophosphate, 1 mM sodium vanadate, 5 mM NaF, and complete protease inhibitors). A minimum of 1 mg of total cellular protein was incubated at 4°C overnight or for 3 h on a rotating wheel with antibody

and complexes, and were then precipitated with 25 µl of protein G–Agarose (Thermo Fisher Scientific) for 20 min on a rotating wheel at 4°C. Beads were washed at least three times in 500 µl of lysis buffer and resuspended in NuPAGE LDS sample buffer before SDS-PAGE. Fluorescent immunoblotting was conducted using the Odyssey infrared scanner according to the manufacturer's protocols (Li-COR Biosciences). Fluorescence data from the Odyssey were exported into Excel. For phosphorylation analysis, signal from phosphospecific antibodies was divided by that of antibodies recognizing total protein (e.g., PY410/Total p130Cas). For p130Cas–Crk complexes, p130Cas signal was divided by Crk signal. For siRNA experiments in tumor cells, data were normalized to values from mock-transfected cells. For HEK 293T cells, data are presented as fold stimulation of phosphorylation, obtained by dividing the phospho/total ratio in uPAR-transfected cells by the vector control. In all cases, statistical comparisons for each siRNA were made against the nontargeting control, and ON-TARGET SMART Pools were compared with ON-TARGET nontargeting controls.

Quantitative PCR
Total cellular RNA was isolated from cultured cells using Trizol (Invitrogen) or the RNeasy Mini kit (QIAGEN). Real-time RT-PCR amplifications were performed using the Brilliant II SYBR Green QRT-PCR Master Mix kit (Stratagene). A standard curve was constructed using a range of 0.01 to 10 ng RNA from BE cells for each set of primers used. Relative quantitation was performed using the $\Delta\Delta C_t$ method. All primers used were Quantitect SYBR green primer assays (QIAGEN). Reactions were performed in triplicate in 50-µl volumes containing 25 µl of 2× Brilliant II mastermix, 5 µl of 10× Quantitect SYBR green primer assay, 1 µl of RT-RNase-block enzyme mixture (Stratagene), and the appropriate amount of RNA with remaining volume made up with nuclease-free water (Ambion). PCR was performed in a Fast Real-Time PCR cycler (7900HT; Applied Biosystems). Data were analyzed using SDS software (Applied Biosystems).

Flow cytometry
Detached cells (5 × 10^6) were stained on ice for 45 min using 10 µg/ml LM609, 10 µg/ml P1F6, or 1 µg/ml P5D2 to detect $\alpha_v\beta_3$, $\alpha_v\beta_5$, and β_1, respectively. Alexa fluor 488–conjugated goat anti–mouse F(ab)$_2$ fragment used for detection (at 1:250) was obtained from Invitrogen. Cells were analyzed on an LSR II flow cytometer (BD Biosciences).

Adhesion assays
Adhesion assays were performed according to the method of Cunningham et al. (2003). Cells were detached by short incubation with trypsin, counted, and washed in serum-free medium. 3 × 10^4 cells were allowed to adhere to 96-well plates (Thermo Fisher Scientific) precoated with 10 µg/ml fibronectin, 2 µg/ml vitronectin, or 10 µg/ml Type-I collagen for 30 min at 37°C. For blocking antibody studies, cells were preincubated with antibodies or control IgG (at 10 µg/ml) for 30 min before addition to the plate. Plates were washed three times in medium containing 0.2% bovine serum albumin (Sigma-Aldrich), fixed in formol saline, and stained with crystal violet. Staining was quantified by measuring absorbance at 540 nm using a SpectraMax M5 (Invitrogen) plate reader.

Online supplemental material
Fig. S1 shows a morphological screen of integrin-associated Rac GEFs. Fig. S2 shows siRNA-mediated knockdown of uPAR, DOCK180, p130Cas, Crk, and integrin subunits. Fig. S3 shows that uPAR-driven Rac activity in 293T cells requires β3 integrin–dependent Src activation. Fig. S4 shows that silencing of β integrin subunits in BE colon carcinoma cells affects cell morphology. Fig. S5 shows that uPAR-driven Rac activation is vitronectin dependent but adhesion to vitronectin requires αvβ3 or αvβ5, but not uPAR. Video 1 shows control BE colon carcinoma cells. Video 2 shows BE colon carcinoma cells transfected with siRNA-targeting uPAR. Video 3 shows BE colon carcinoma cells transfected with siRNA-targeting DOCK180. Online supplemental material is available at http://www.jcb.org/cgi/content/full/jcb.200712050/DC1.

References

Aguirre Ghiso, J.A. 2002. Inhibition of FAK signaling activated by urokinase receptor induces dormancy in human carcinoma cells in vivo. *Oncogene.* 21:2513–2524.

Aguirre-Ghiso, J.A. 2007. Models, mechanisms and clinical evidence for cancer dormancy. *Nat. Rev. Cancer.* 7:834–846.

Aguirre Ghiso, J.A., K. Kovalski, and L. Ossowski. 1999. Tumor dormancy induced by downregulation of urokinase receptor in human carcinoma involves integrin and MAPK signaling. *J. Cell Biol.* 147:89–104.

Arthur, W.T., L.A. Quilliam, and J.A. Cooper. 2004. Rap1 promotes cell spreading by localizing Rac guanine nucleotide exchange factors. *J. Cell Biol.* 167:111–122.

Auvinen, M., A. Paasinen-Sohns, H. Hirai, L.C. Andersson, and E. Holtta. 1995. Ornithine decarboxylase- and ras-induced cell transformations: reversal by protein tyrosine kinase inhibitors and role of pp130CAS. *Mol. Cell. Biol.* 15:6513–6525.

Bass, R., F. Werner, E. Odintsova, T. Sugiura, F. Berditchevski, and V. Ellis. 2005. Regulation of urokinase receptor proteolytic function by the tetraspanin CD82. *J. Biol. Chem.* 280:14811–14818.

Behrendt, N., O.N. Jensen, L.H. Engelholm, E. Mortz, M. Mann, and K. Dano. 2000. A urokinase receptor-associated protein with specific collagen binding properties. *J. Biol. Chem.* 275:1993–2002.

Benard, V., B.P. Bohl, and G.M. Bokoch. 1999. Characterization of rac and cdc42 activation in chemoattractant-stimulated human neutrophils using a novel assay for active GTPases. *J. Biol. Chem.* 274:13198–13204.

Bene, M.C., G. Castoldi, W. Knapp, G.M. Rigolin, L. Escribano, P. Lemez, W.D. Ludwig, E. Matutes, A. Orfao, F. Lanza, and M. van't Veer. 2004. CD87 (urokinase-type plasminogen activator receptor), function and pathology in hematological disorders: a review. *Leukemia.* 18:394–400.

Bershadsky, A., M. Kozlov, and B. Geiger. 2006. Adhesion-mediated mechano-sensitivity: a time to experiment, and a time to theorize. *Curr. Opin. Cell Biol.* 18:472–481.

Blasi, F., and P. Carmeliet. 2002. uPAR: a versatile signalling orchestrator. *Nat. Rev. Mol. Cell Biol.* 3:932–943.

Bos, J.L., H. Rehmann, and A. Wittinghofer. 2007. GEFs and GAPs: critical elements in the control of small G proteins. *Cell.* 129:865–877.

Brugnera, E., L. Haney, C. Grimsley, M. Lu, S.F. Walk, A.C. Tosello-Trampont, I.G. Macara, H. Madhani, G.R. Fink, and K.S. Ravichandran. 2002. Unconventional Rac-GEF activity is mediated through the Dock180-ELMO complex. *Nat. Cell Biol.* 4:574–582.

Cabodi, S., A. Tinnirello, P. Di Stefano, B. Bisaro, E. Ambrosino, I. Castellano, A. Sapino, R. Arisio, F. Cavallo, G. Forni, et al. 2006. p130Cas as a new regulator of mammary epithelial cell proliferation, survival, and HER2-neu oncogene-dependent breast tumorigenesis. *Cancer Res.* 66:4672–4680.

Carriero, M.V., S. Del Vecchio, M. Capozzoli, P. Franco, L. Fontana, A. Zannetti, G. Botti, G. D'Aiuto, M. Salvatore, and M.P. Stoppelli. 1999. Urokinase receptor interacts with alpha(v)beta5 vitronectin receptor, promoting urokinase-dependent cell migration in breast cancer. *Cancer Res.* 59:5307–5314.

Chaurasia, P., J.A. Aguirre-Ghiso, O.D. Liang, H. Gardsvoll, M. Ploug, and L. Ossowski. 2006. A region in urokinase plasminogen receptor domain III controlling a functional association with alpha5beta1 integrin and tumor growth. *J. Biol. Chem.* 281:14852–14863.

Cheresh, D.A., and R.C. Spiro. 1987. Biosynthetic and functional properties of an Arg-Gly-Asp-directed receptor involved in human melanoma cell attachment to vitronectin, fibrinogen, and von Willebrand factor. *J. Biol. Chem.* 262:17703–17711.

Cunningham, O., A. Andolfo, M.L. Santovito, L. Iuzzolino, F. Blasi, and N. Sidenius. 2003. Dimerization controls the lipid raft partitioning of uPAR/CD87 and regulates its biological functions. *EMBO J.* 22:5994–6003.

Czekay, R.-P., T.A. Kuemmel, R.A. Orlando, and M.G. Farquhar. 2001. Direct binding of occupied urokinase receptor (uPAR) to LDL receptor-related protein is required for endocytosis of uPAR and regulation of cell surface urokinase activity. *Mol. Biol. Cell.* 12:1467–1479.

Dano, K., N. Behrendt, G. Hoyer-Hansen, M. Johnsen, L.R. Lund, M. Ploug, and J. Romer. 2005. Plasminogen activation and cancer. *Thromb. Haemost.* 93:676–681.

Degryse, B., M. Resnati, R.P. Czekay, D.J. Loskutoff, and F. Blasi. 2005. Domain 2 of the urokinase receptor contains an integrin-interacting epitope with intrinsic signaling activity: generation of a new integrin inhibitor. *J. Biol. Chem.* 280:24792–24803.

Del Pozo, M.A., W.B. Kiosses, N.B. Alderson, N. Meller, K.M. Hahn, and M.A. Schwartz. 2002. Integrins regulate GTP-Rac localized effector interactions through dissociation of Rho-GDI. *Nat. Cell Biol.* 4:232–239.

del Pozo, M.A., N.B. Alderson, W.B. Kiosses, H.H. Chiang, R.G. Anderson, and M.A. Schwartz. 2004. Integrins regulate Rac targeting by internalization of membrane domains. *Science.* 303:839–842.

El-Kott, A.F., A.M. Khalil, and M. El-Kenawy Ael. 2004. Immunohistochemical expressions of uPA and its receptor uPAR and their prognostic significant in urinary bladder carcinoma. *Int. Urol. Nephrol.* 36:417–423.

Etienne-Manneville, S. 2004. Cdc42—the centre of polarity. *J. Cell Sci.* 117:1291–1300.

Faccio, R., S.L. Teitelbaum, K. Fujikawa, J. Chappel, A. Zallone, V.L. Tybulewicz, F.P. Ross, and W. Swat. 2005. Vav3 regulates osteoclast function and bone mass. *Nat. Med.* 11:284–290.

Gakidis, M.A., X. Cullere, T. Olson, J.L. Wilsbacher, B. Zhang, S.L. Moores, K. Ley, W. Swat, T. Mayadas, and J.S. Brugge. 2004. Vav GEFs are required for β₂ integrin-dependent functions of neutrophils. *J. Cell Biol.* 166:273–282.

Gumienny, T.L., E. Brugnera, A.C. Tosello-Trampont, J.M. Kinchen, L.B. Haney, K. Nishiwaki, S.F. Walk, M.E. Nemergut, I.G. Macara, R. Francis, et al. 2001. CED-12/ELMO, a novel member of the CrkII/Dock180/Rac pathway, is required for phagocytosis and cell migration. *Cell.* 107:27–41.

Hamelers, I.H., C. Olivo, A.E. Mertens, D.M. Pegtel, R.A. van der Kammen, A. Sonnenberg, and J.G. Collard. 2005. The Rac activator Tiam1 is required for α3β1-mediated laminin-5 deposition, cell spreading, and cell migration. *J. Cell Biol.* 171:871–881.

Honda, H., H. Oda, T. Nakamoto, Z. Honda, R. Sakai, T. Suzuki, T. Saito, K. Nakamura, K. Nakao, T. Ishikawa, et al. 1998. Cardiovascular anomaly, impaired actin bundling and resistance to Src-induced transformation in mice lacking p130Cas. *Nat. Genet.* 19:361–365.

Jaffe, A.B., and A. Hall. 2005. Rho GTPases: biochemistry and biology. *Annu. Rev. Cell Dev. Biol.* 21:247–269.

Jo, M., K.S. Thomas, D.M. O'Donnell, and S.L. Gonias. 2003. Epidermal growth factor receptor-dependent and -independent cell-signaling pathways originating from the urokinase receptor. *J. Biol. Chem.* 278:1642–1646.

Jo, M., K.S. Thomas, S. Takimoto, A. Gaultier, E.H. Hsieh, R.D. Lester, and S.L. Gonias. 2006. Urokinase receptor primes cells to proliferate in response to epidermal growth factor. *Oncogene.* 26:2585–2594.

Kaneko, T., H. Konno, M. Baba, T. Tanaka, and S. Nakamura. 2003. Urokinase-type plasminogen activator expression correlates with tumor angiogenesis and poor outcome in gastric cancer. *Cancer Sci.* 94:43–49.

Kirsch, K., M. Kensinger, H. Hanafusa, and A. August. 2002. A p130Cas tyrosine phosphorylated substrate domain decoy disrupts v-crk signaling. *BMC Cell Biol.* 3:18.

Kiyokawa, E., Y. Hashimoto, T. Kurata, H. Sugimura, and M. Matsuda. 1998. Evidence that DOCK180 up-regulates signals from the CrkII-p130(Cas) complex. *J. Biol. Chem.* 273:24479–24484.

Kjoller, L., and A. Hall. 2001. Rac mediates cytoskeletal rearrangements and increased cell motility induced by urokinase-type plasminogen activator receptor binding to vitronectin. *J. Cell Biol.* 152:1145–1157.

Klemke, R.L., J. Leng, R. Molander, P.C. Brooks, K. Vuori, and D.A. Cheresh. 1998. CAS/Crk coupling serves as a "molecular switch" for induction of cell migration. *J. Cell Biol.* 140:961–972.

Lester, R.D., M. Jo, V. Montel, S. Takimoto, and S.L. Gonias. 2007. uPAR induces epithelial–mesenchymal transition in hypoxic breast cancer cells. *J. Cell Biol.* 178:425–436.

Liu, D., J. Aguirre Ghiso, Y. Estrada, and L. Ossowski. 2002. EGFR is a transducer of the urokinase receptor initiated signal that is required for in vivo growth of a human carcinoma. *Cancer Cell.* 1:445–457.

Llinas, P., M.H. Le Du, H. Gardsvoll, K. Dano, M. Ploug, B. Gilquin, E.A. Stura, and A. Menez. 2005. Crystal structure of the human urokinase plasminogen activator receptor bound to an antagonist peptide. *EMBO J.* 24:1655–1663.

Ma, Z., K.S. Thomas, D.J. Webb, R. Moravec, A.M. Salicioni, W.M. Mars, and S.L. Gonias. 2002. Regulation of Rac1 activation by the low density lipoprotein receptor–related protein. *J. Cell Biol.* 159:1061–1070.

Madsen, C.D., G.M. Ferraris, A. Andolfo, O. Cunningham, and N. Sidenius. 2007. uPAR-induced cell adhesion and migration: vitronectin provides the key. *J. Cell Biol.* 177:927–939.

Marignani, P.A., and C.L. Carpenter. 2001. Vav2 is required for cell spreading. *J. Cell Biol.* 154:177–186.

Matsuda, M., S. Ota, R. Tanimura, H. Nakamura, K. Matuoka, T. Takenawa, K. Nagashima, and T. Kurata. 1996. Interaction between the amino-terminal SH3 domain of CRK and its natural target proteins. *J. Biol. Chem.* 271:14468–14472.

Matsuo, N., M. Terao, Y.-i. Nabeshima, and M. Hoshino. 2003. Roles of STEF/Tiam1, guanine nucleotide exchange factors for Rac1, in regulation of growth cone morphology. *Mol. Cell. Neurosci.* 24:69–81.

Memarzadeh, S., K.R. Kozak, L. Chang, S. Natarajan, P. Shintaku, S.T. Reddy, and R. Farias-Eisner. 2002. Urokinase plasminogen activator receptor: prognostic biomarker for endometrial cancer. *Proc. Natl. Acad. Sci. USA.* 99:10647–10652.

Meng, S., D. Tripathy, S. Shete, R. Ashfaq, H. Saboorian, B. Haley, E. Frenkel, D. Euhus, M. Leitch, C. Osborne, et al. 2006. uPAR and HER-2 gene status in individual breast cancer cells from blood and tissues. *Proc. Natl. Acad. Sci. USA.* 103:17361–17365.

Mohan, P.M., S.K. Chintala, S. Mohanam, C.L. Gladson, E.S. Kim, Z.L. Gokaslan, S.S. Lakka, J.A. Roth, B. Fang, R. Sawaya, et al. 1999. Adenovirus-mediated delivery of antisense gene to urokinase-type plasminogen activator receptor suppresses glioma invasion and tumor growth. *Cancer Res.* 59:3369–3373.

Moore, C.A., C.A. Parkin, Y. Bidet, and P.W. Ingham. 2007. A role for the Myoblast city homologues Dock1 and Dock5 and the adaptor proteins Crk and Crk-like in zebrafish myoblast fusion. *Development.* 134:3145–3153.

Moores, S.L., L.M. Selfors, J. Fredericks, T. Breit, K. Fujikawa, F.W. Alt, J.S. Brugge, and W. Swat. 2000. Vav family proteins couple to diverse cell surface receptors. *Mol. Cell. Biol.* 20:6364–6373.

Nievers, M.G., R.B. Birge, H. Greulich, A.J. Verkleij, H. Hanafusa, and P.M. van Bergen en Henegouwen. 1997. v-Crk-induced cell transformation: changes in focal adhesion composition and signaling. *J. Cell Sci.* 110:389–399.

Nolan, K.M., K. Barrett, Y. Lu, K.Q. Hu, S. Vincent, and J. Settleman. 1998. Myoblast city, the *Drosophila* homolog of DOCK180/CED-5, is required in a Rac signaling pathway utilized for multiple developmental processes. *Genes Dev.* 12:3337–3342.

Pedersen, N., M. Schmitt, E. Ronne, M.I. Nicoletti, G. Hoyer-Hansen, M. Conese, R. Giavazzi, K. Dano, W. Kuhn, F. Janicke, et al. 1993. A ligand-free, soluble urokinase receptor is present in the ascitic fluid from patients with ovarian cancer. *J. Clin. Invest.* 92:2160–2167.

Pollard, T.D., and G.G. Borisy. 2003. Cellular motility driven by assembly and disassembly of actin filaments. *Cell.* 112:453–465.

Polte, T.R., and S.K. Hanks. 1995. Interaction between focal adhesion kinase and Crk-associated tyrosine kinase substrate p130Cas. *Proc. Natl. Acad. Sci. USA.* 92:10678–10682.

Pyke, C., J. Eriksen, H. Solberg, B.S. Nielsen, P. Kristensen, L.R. Lund, and K. Dano. 1993. An alternatively spliced variant of mRNA for the human receptor for urokinase plasminogen activator. *FEBS Lett.* 326:69–74.

Resnati, M., I. Pallavicini, J.M. Wang, J. Oppenheim, C.N. Serhan, M. Romano, and F. Blasi. 2002. The fibrinolytic receptor for urokinase activates the G protein-coupled chemotactic receptor FPRL1/LXA4R. *Proc. Natl. Acad. Sci. USA.* 99:1359–1364.

Ribatti, D., D. Leali, A. Vacca, R. Giuliani, A. Gualandris, L. Roncali, M.L. Nolli, and M. Presta. 1999. In vivo angiogenic activity of urokinase: role of endogenous fibroblast growth factor-2. *J. Cell Sci.* 112:4213–4221.

Rosenberger, G., I. Jantke, A. Gal, and K. Kutsche. 2003. Interaction of aPIX (ARHGEF6) with b-parvin (PARVB) suggests an involvement of aPIX in integrin-mediated signaling. *Hum. Mol. Genet.* 12:155–167.

Sakai, R., A. Iwamatsu, N. Hirano, S. Ogawa, T. Tanaka, H. Mano, Y. Yazaki, and H. Hirai. 1994. A novel signaling molecule, p130, forms stable complexes in vivo with v-Crk and v-Src in a tyrosine phosphorylation-dependent manner. *EMBO J.* 13:3748–3756.

Saksela, O., and D.B. Rifkin. 1990. Release of basic fibroblast growth factor-heparan sulfate complexes from endothelial cells by plasminogen activator-mediated proteolytic activity. *J. Cell Biol.* 110:767–775.

Salajegheh, M., A. Rudnicki, and T.W. Smith. 2005. Expression of urokinase-type plasminogen activator receptor (uPAR) in primary central nervous system neoplasms. *Appl. Immunohistochem. Mol. Morphol.* 13:184–189.

Sato, Y., R. Tsuboi, R. Lyons, H. Moses, and D.B. Rifkin. 1990. Characterization of the activation of latent TGF-beta by co-cultures of endothelial cells and pericytes or smooth muscle cells: a self-regulating system. *J. Cell Biol.* 111:757–763.

Sawada, Y., M. Tamada, B.J. Dubin-Thaler, O. Cherniavskaya, R. Sakai, S. Tanaka, and M.P. Sheetz. 2006. Force sensing by mechanical extension of the Src family kinase substrate p130Cas. *Cell.* 127:1015–1026.

Schvartz, I., D. Seger, and S. Shaltiel. 1999. Vitronectin. *Int. J. Biochem. Cell Biol.* 31:539–544.

Sidenius, N., A. Andolfo, R. Fesce, and F. Blasi. 2002. Urokinase regulates vitronectin binding by controlling urokinase receptor oligomerization. *J. Biol. Chem.* 277:27982–27990.

Simon, D.I., N.K. Rao, H. Xu, Y. Wei, O. Majdic, E. Ronne, L. Kobzik, and H.A. Chapman. 1996. Mac-1 (CD11b/CD18) and the urokinase receptor (CD87) form a functional unit on monocytic cells. *Blood.* 88:3185–3194.

Sturge, J., J. Hamelin, and G.E. Jones. 2002. N-WASP activation by a beta1-integrin-dependent mechanism supports PI3K-independent chemotaxis stimulated by urokinase-type plasminogen activator. *J. Cell Sci.* 115:699–711.

Tosello-Trampont, A.C., J.M. Kinchen, E. Brugnera, L.B. Haney, M.O. Hengartner, and K.S. Ravichandran. 2007. Identification of two signaling

submodules within the CrkII/ELMO/Dock180 pathway regulating engulf-ment of apoptotic cells. *Cell Death Differ.* 14:963–972.

Vial, E., E. Sahai, and C.J. Marshall. 2003. ERK-MAPK signaling coordinately regulates activity of Rac1 and RhoA for tumor cell motility. *Cancer Cell.* 4:67–79.

Vuori, K., H. Hirai, S. Aizawa, and E. Ruoslahti. 1996. Introduction of p130cas signaling complex formation upon integrin-mediated cell adhesion: a role for Src family kinases. *Mol. Cell. Biol.* 16:2606–2613.

Wei, C., C.C. Moller, M.M. Altintas, J. Li, K. Schwarz, S. Zacchigna, L. Xie, A. Henger, H. Schmid, M.P. Rastaldi, et al. 2008. Modification of kidney barrier function by the urokinase receptor. *Nat. Med.* 14:55–63.

Wei, Y., D.A. Waltz, N. Rao, R.J. Drummond, S. Rosenberg, and H.A. Chapman. 1994. Identification of the urokinase receptor as an adhesion receptor for vitronectin. *J. Biol. Chem.* 269:32380–32388.

Wei, Y., J.A. Eble, Z. Wang, J.A. Kreidberg, and H.A. Chapman. 2001. Urokinase receptors promote beta1 integrin function through interactions with inte-grin alpha3beta1. *Mol. Biol. Cell.* 12:2975–2986.

Wei, Y., R.P. Czekay, L. Robillard, M.C. Kugler, F. Zhang, K.K. Kim, J.P. Xiong, M.J. Humphries, and H.A. Chapman. 2005. Regulation of α5β1 integrin conformation and function by urokinase receptor binding. *J. Cell Biol.* 168:501–511.

Wei, Y., C.H. Tang, Y. Kim, L. Robillard, F. Zhang, M.C. Kugler, and H.A. Chapman. 2007. Urokinase receptors are required for alpha 5 beta 1 integrin-mediated signaling in tumor cells. *J. Biol. Chem.* 282:3929–3939.

Woods, D., H. Cherwinski, E. Venetsanakos, A. Bhat, S. Gysin, M. Humbert, P.F. Bray, V.L. Saylor, and M. McMahon. 2001. Induction of beta3-integrin gene expression by sustained activation of the Ras-regulated Raf-MEK-extracellular signal-regulated kinase signaling pathway. *Mol. Cell. Biol.* 21:3192–3205.

Wu, Y.C., and H.R. Horvitz. 1998. *C. elegans* phagocytosis and cell-migration protein CED-5 is similar to human DOCK180. *Nature.* 392:501–504.

Xue, W., I. Mizukami, R.F. Todd III, and H.R. Petty. 1997. Urokinase-type plasminogen activator receptors associate with beta1 and beta3 integrins of fibrosarcoma cells: dependence on extracellular matrix components. *Cancer Res.* 57:1682–1689.

Zanetti, A., G. Conforti, S. Hess, I. Martin-Padura, E. Ghibaudi, K.T. Preissner, and E. Dejana. 1994. Clustering of vitronectin and RGD peptides on microspheres leads to engagement of integrins on the luminal aspect of endothelial cell membrane. *Blood.* 84:1116–1123.

Zhang, F., C.C. Tom, M.C. Kugler, T.T. Ching, J.A. Kreidberg, Y. Wei, and H.A. Chapman. 2003. Distinct ligand binding sites in integrin α3β1 regulate matrix adhesion and cell–cell contact. *J. Cell Biol.* 163:177–188.